THE JOURNAL OF PHYSICAL CHEMISTRY B

Article

Cite This: J. Phys. Chem. B 2019, 123, 5412−5422

pubs.acs.org/JPCB

Novel Heat-Promoted Folding Dynamics of the *yybP-ykoY* Manganese Riboswitch: Kinetic and Thermodynamic Studies at the Single-Molecule Level

Hsuan-Lei Sung[†] and David J. Nesbitt*[,‡,§]

[†]JILA, Department of Chemistry, and [§]Department of Physics, University of Colorado, Boulder, Colorado 80309, United States

[‡]JILA, National Institute of Standards and Technology and University of Colorado, Boulder, Colorado 80309, United States

ABSTRACT: Riboswitches are highly structured RNA elements that regulate gene expressions by undergoing conformational changes in response to their cognate ligands. Such regulatory strategies are particularly prevalent among bacteria, which need to be evolutionarily responsive to thermal fluctuations in the surrounding environment, for example, generating extremophiles evolved to survive anomalously high or low temperatures. As a consequence, the response of such riboswitches to thermal stress becomes of considerable interest. In this study, the temperature-dependent folding kinetics and thermodynamics of the manganese riboswitch (*yybP-ykoY*) is studied by single-molecule FRET spectroscopy under external thermal control. Surprisingly, the *folding* of the manganese riboswitch is found to be strongly *promoted* by temperature. Detailed thermodynamic analysis of the equilibrium and forward/reverse kinetic rate constants reveal folding to be a strongly endothermic process (ΔH^0) made feasible by an overall entropic lowering ($-T\Delta S^0$) in free energy. This is in contrast to a more typical picture of RNA folding achieving a more compact, highly ordered state (ΔS^0) and clearly speaks to the significant role of solvent/cation reorganization in the folding thermodynamics. With the help of the transition-state theory, free energy landscapes for the manganese riboswitch are constructed from the temperature-dependent kinetic data, revealing two distinctive folding mechanisms promoted by Mg^{2+} and Mn^{2+}, respectively. It is speculated that this unconventional temperature dependence for folding of the manganese riboswitch may reflect evolution of bacterial gene regulation strategies to survive environments with large-temperature variations.

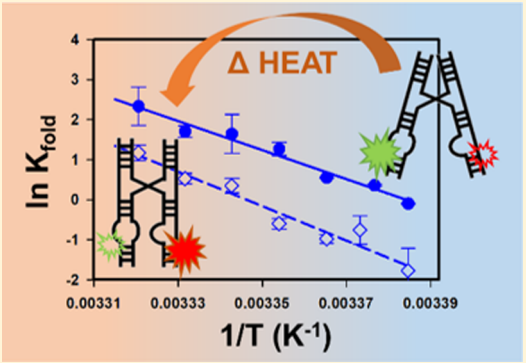

1. INTRODUCTION

Riboswitches are noncoding mRNA elements that regulate gene expression by undergoing conformational changes upon ligand binding.[1−3] These riboswitches are particularly widely exploited in bacterial gene regulation, responding to a wide variety of ligands including small-molecule metabolites and atomic ions.[4,5] The structure of a riboswitch is typically comprised of an aptamer domain and an expression platform.[5,6] The aptamer domain of a riboswitch structurally conforms to selectively capture its cognate ligand, while the expression platform adopts a distinctive folding structure in response to the aptamer. Such complex conformational transitions result in clear "on" and "off" states of a riboswitch,[6] which can structurally regulate downstream gene expression. Common regulatory strategies include premature transcriptional termination and blocked translation initiation.[4,5]

Temperature is known to significantly influence the biomolecular structure and, consequently, biochemical function. Folding into a more ordered RNA structure typically results in a state of lower entropy[7,8] ($-T\Delta S^0$) with the net folding enthalpically driven (ΔH^0) by interactions such as hydrogen bonding and charge neutralization.[9,10] By Le Chatelier's principle, such enthalpically driven processes give rise to strongly temperature-dependent equilibrium and kinetic behavior. The requisite exothermicity for such structure formation, in turn, is routinely observed and confirmed in many examples of thermal denaturation, whereby biomolecules unfold from their native structures with elevated temperature.[11,12] However, in contrast to more of these conventional pictures of folding, some biomolecules are found to *unfold* with *decreasing* temperature, that is, so called "heat-promoted folding" or, equivalently, "cold denaturation".[13,14] Such reversal in the normal paradigmatic behavior can arise, for example, from changes in the solvent configurations dominated by hydrophobic and hydrophilic interactions, which also contribute significantly to the overall free energy and thereby influence the thermal sensitivity of biomolecular folding.[7,15,16] In the case of cold denaturation, it is the entropic gain in solvent configuration which overcomes any entropic penalty associated with a more compact structure, thus providing a predominantly entropic driving force for biomolecular folding.

Received: March 27, 2019
Revised: May 2, 2019
Published: June 6, 2019

DOI: 10.1021/acs.jpcb.9b02852
J. Phys. Chem. B 2019, 123, 5412−5422

Unlike many proteins which function from a native folded state, riboswitches regulate gene expression dynamically by switching between on and off configurations in response to cellular environment and ligand association. As the two different conformational states result in opposite biochemical outcomes, it is reasonable to expect gene regulation by riboswitches to be modulated by temperature. However, exactly how a riboswitch reacts to thermal stress remains unclear because both on- and off-state conformations each contain complex secondary and tertiary structural motifs. This provides important motivation for exploring temperature-dependent dynamics of riboswitch folding as well as consideration of any potential evolutionary advantages. Given that bacteria can experience significant temperature fluctuations in their environment and indeed some may even endure high or low extremes,[17−19] it is not surprising that they may have evolved to incorporate thermal stress as an important element in gene regulation strategies.[20−23] In fact, some temperature-responsive RNA motifs commonly referred to as "RNA thermometers" have been discovered.[22,23] Similar to riboswitches, they often regulate genes related to heat shock response by a thermally responsive conformational change. The results of the present study take this concept one step further, suggesting that temperature modulation might be a common feature of riboswitch gene regulation and thus potentially a more general protective mechanism for bacteria under thermal fluctuations and/or biochemical distress.

The particular focus of this work is the manganese riboswitch, which is found to be extensively distributed in the noncoding regions of bacterial mRNA.[24−26] It responds to micromolar concentration of cellular Mn^{2+} and regulates the expression of genes responsible for metal homeostasis, including the manganese efflux pump, a transport protein that removes excess Mn^{2+} from the cell.[27−29] The aptamer domain of manganese riboswitch consists of four helices tethered by a four-way junction (Figure 1A,C). In the ligand-bound-folded state identified in previous X-ray studies[25] (Figure 1A), the four helices coaxially align into a tight hairpin-like structure with docking between two highly conserved loops L1 and L3. The docking interface formed by L1 and L3 contains one Mn^{2+} specific binding site and one nonselective divalent cation M^{2+} (M = Mn or Mg) binding site that is predominantly occupied by Mg^{2+} by natural physiological abundance (Figure 1B). Regulation of gene expression can therefore be activated by single-metal ion (M^{2+}) binding, followed by L1 and L3 docking.

In this study, thermal response of the manganese riboswitch is studied by single-molecule FRET (smFRET) spectroscopy and kinetics under external temperature control (±0.1 °C), where conformational folding of a single RNA molecule is monitored by FRET energy transfer efficiency (E_{FRET}) as a function of time. The resulting E_{FRET} time trajectories not only explicitly recapitulate the *equilibrium* folding behavior but also contain detailed information on single-molecule *kinetics* for further analysis of the unimolecular folding/unfolding rate processes. Indeed, it has long been recognized that "co-transcriptional formation" of the natively folded riboswitch structure is a crucial strategic element in real-time gene regulation.[1,30,31] Thus, the kinetic time scales for manganese riboswitch folding and unfolding become particularly important to ensuring an adequate temporal window for both (i) metabolite recognition and (ii) conformational change with respect to the gene transcription-regulated event.

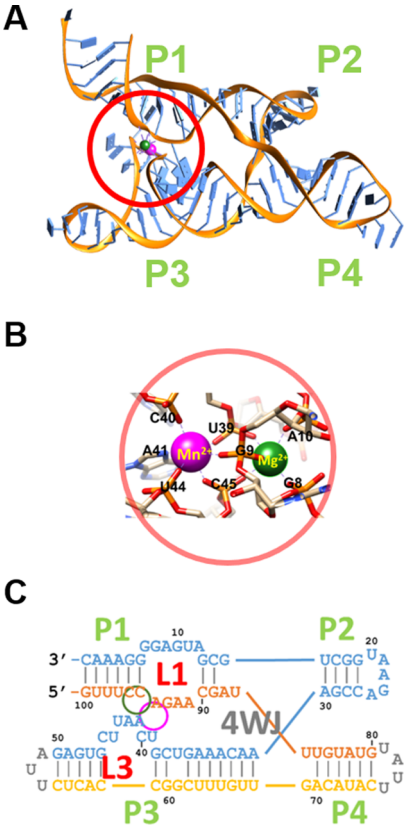

Figure 1. Structure of *L. lactis yybP-ykoY* manganese riboswitch. (A) Overall crystal structure (PDB 4Y1I); (B) close-up details on the cation M^{2+} binding sites with adjacent nucleotides; (C) manganese riboswitch sequence in secondary structure representation.

In our investigation of such temperature-dependent manganese riboswitch dynamics, we find that the folding kinetics is strongly sensitive to and increases dramatically with temperature. Thermodynamic analysis of the single-molecule data as a function of temperature allows us to decompose the folding free energy into entropic and enthalpic contributions, revealing that manganese riboswitch folding is surprisingly endothermic and compensated by favorable entropic gain. With the help of such thermodynamic and kinetic data, a detailed energy landscape of manganese riboswitch folding can be reconstructed from transition-state (TS) theory, highlighting several intriguing observations consistent with our previous kinetic study of manganese riboswitch folding mechanisms.[32] Specifically, the manganese riboswitch is found to respond to Mg^{2+} primarily during the early stages of folding and prior to surmounting the TS barrier. This is in agreement with a "bind-then-fold" (i.e., induced fit or IF) mechanism, whereby folding is directly promoted by Mg^{2+} association. Mn^{2+}, on the other hand, changes free energies in both early and late stages of folding, implying that different M^{2+} (M = Mn or Mg) occupancies can be adopted in the folded manganese riboswitch. This is in support of the "fold-then-bind" (i.e., conformation selection or CS) mechanism, whereby the ligand binds to and thermodynamically stabilizes an already preorganized fold-like structure.[30,32,33]

2. EXPERIMENT

2.1. RNA Construct Design and Preparation for the Single-Molecule Study. The ligand-bound folded state of

DOI: 10.1021/acs.jpcb.9b02852
J. Phys. Chem. B 2019, 123, 5412−5422

the manganese riboswitch has been determined in previous X-ray studies to be a hairpin-like structure formed from four jointed helices (Figure 1A).[25] The major docking interaction between L1 and L3 directly responds to M^{2+} ligand binding, which is crucial to stabilizing the folded conformation. Therefore, we have designed a smFRET RNA construct sensitive to the distance between L1 and L3 as a proxy for conformational change.[32] In this smFRET construct design, the cyanine dyes Cy3 and Cy5 are covalently labeled on P1 and P3 stems, respectively, to achieve two distinct distance-dependent energy transfer states distinguished by RNA folding/unfolding (Figure 2A). Biotin modification is introduced to the P1 end so that the RNA construct can be tethered on a coverslip surface by biotin−streptavidin interactions for study at the single-molecule level. The Mn^{2+} aptamer domain is reconstructed from the RNA sequence in *Lactococcus lactis*, as structurally characterized in previous studies.[25,32] The final smFRET manganese riboswitch construct is synthesized by annealing three chemically modified RNA oligos purchased from Integrated DNA Technologies (IDT, Coralville, IA), followed by high-performance liquid chromatography purification. Detailed construct design and explicit oligo sequences can be found in our previous work.[32]

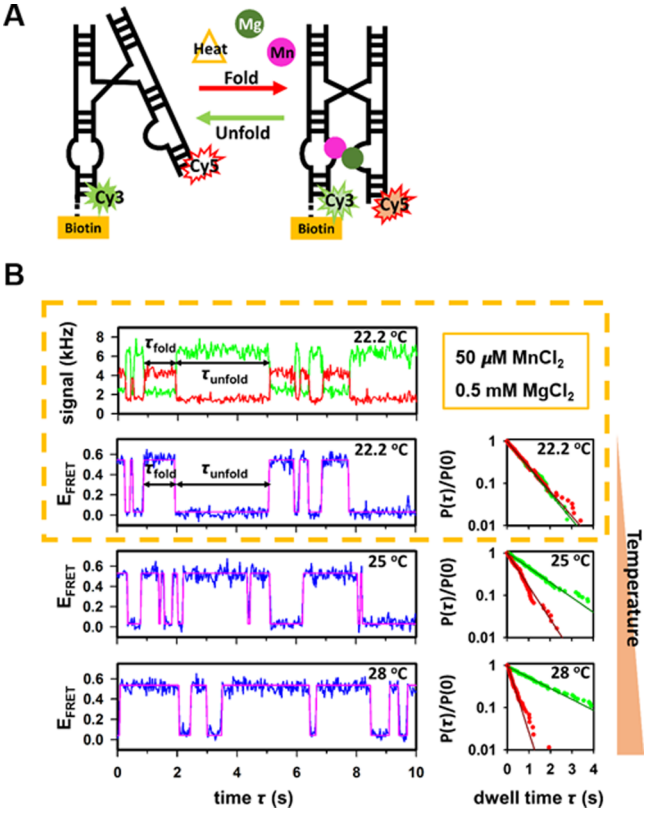

Figure 2. Sample smFRET experiment data. (A) Cartoon depiction of how manganese riboswitch folding changes the distance between Cy3 and Cy5; (B) sample time trace of Cy3 and Cy5 fluorescence (22.2 °C, top left), the corresponding E_{FRET} trajectory (lower left), and a series of E_{FRET} trajectories (lower left) and dwell time distributions (lower right) as a function of increasing temperature (22.2−28.0 °C). Note that a small increase in temperature dramatically increases the folded time distributions, consistent with strong endothermic folding (ΔH^0).

By way of sample preparation for these smFRET experiments, the sample holder is flushed in sequential order with (i) 10 mg/mL bovine serum albumin with 10% biotinylation for surface pacification, (ii) 200 μg/mL streptavidin for surface tethering, and (iii) ∼25 pM of the biotinylated RNA construct. Each flushing step is followed by a 10 min incubation period, which yields a consistent, reliable surface coverage of ∼50 RNAs per 100 μm^2. In addition to the specified Mn^{2+} ($MnCl_2$) and Mg^{2+} ($MgCl_2$) divalent cation concentrations, the smFRET buffer solution also contains (i) 50 mM hemisodium *N*-(2-hydroxyethyl)piperazine-*N*′-ethanesulfonic acid (HEPES, pH 7.5), (ii) an enzymatic oxygen scavenger system (PCD/PCA/TROLOX), and (iii) 100 mM NaCl background salt.

2.2. smFRET Spectroscopy. Single-molecule fluorescence imaging capabilities are achieved in a homebuilt confocal microscope system described in previous papers.[34,35] In short, a 532 nm pulsed Nd:YAG laser is collimated by a Keplerian beam expander before being directed into an inverted microscope water immersion objective (1.2 N.A.), resulting in a diffraction-limited laser excitation spot of ∼250 nm lateral dimension. In smFRET experiments, the dye-labeled RNA molecules are located by scanning the coverslip surface under conditions where RNA coverage is sufficiently low to ensure observation of one RNA molecule at a time in the sub-femtoliter confocal volume. The fluorescence photon from a single dye-labeled RNA is collected for each pulse through the same microscope objective and split into color (green/red) and polarization (horizontal/vertical) channels before detection by four single-photon avalanche photodiodes. For each photon event, the color, polarization, wall clock time (±50 ns), and time, respect to the laser pulse (±50 ps) are recorded by a time-correlated single-photon counting module.[35,36] For temperature-controlled studies, thermal equilibrium at a desired temperature (±0.1 °C) is achieved by heating both sample and microscope objective simultaneously, with details of the commercial stage and objective heater setup presented in previous work.[34−36] Before each experimental temperature run, samples remain in contact with the objective for >15 min to ensure complete thermal equilibrium.

3. RESULTS AND ANALYSIS

3.1. Temperature-Promoted Folding Revealed by smFRET. The smFRET RNA construct is doubly labeled with fluorophores Cy3 and Cy5 so that the conformational change can be visualized by distance-dependent FRET energy transfer (E_{FRET}).[32] In the sample fluorescence signal time trace (Figure 2B upper panel), the clearly anticorrelated switching between the donor (green) and acceptor (red) signals unambiguously reflects folding/unfolding events and energy transfer between Cy3 and Cy5, from which the corresponding time-dependent E_{FRET} trajectory can be calculated. The resulting time trace for E_{FRET} (see Figure 2B) reveals that the RNA construct switches between two distinct states with well-separated E_{FRET} values of ∼0.55 and ∼0. As expected from construct geometry[32] and crystal structure data,[25] the high E_{FRET} state ($E_{FRET} \approx 0.55$) corresponds to a compact folded conformation of the manganese riboswitch with loops L1 and L3 docking onto each other. Conversely, the low E_{FRET} is consistent with the two loops much further apart, corresponding to a noncompact, unfolded conformation.

From the E_{FRET} trajectory, the folding equilibrium constant (K_{eq}) can be readily obtained from the ratio of total time spent in the high E_{FRET} (folded) versus low E_{FRET} (unfolded) state.

DOI: 10.1021/acs.jpcb.9b02852
J. Phys. Chem. B 2019, 123, 5412−5422

More revealingly, however, direct observation of the dynamic folding/unfolding behavior also permits the rate constants (k_{fold} and k_{unfold}) to be determined by analysis of the corresponding dwell time distributions (Figure 2B right panels).[32,35] Specifically, semilogarithmic plots of the resulting cumulative distribution functions ($P(\tau)/P(0)$) versus dwell times are linear and thus appropriately fit to a single exponential decay function to extract the first-order folding/unfolding rate constants (k_{fold} and k_{unfold}).

In the temperature-dependent studies, the temperature is controlled (±0.1 °C) by simultaneously heating the sample and the optical objective. A representative temperature response of the manganese riboswitch is illustrated in the series of E_{FRET} trajectories obtained at increasing thermal stress (Figure 2B from top to bottom), for which the RNA clearly spends more time in the high E_{FRET} (i.e., folded) state. Indeed, the approximately 5-fold increase in K_{eq} for ΔT =+5.8 °C indicates that folding of the manganese riboswitch is both highly sensitive to temperature and favored by heat. In addition, the dwell time analysis (Figure 2B right) reveals the kinetic origin of such "heat-promoted folding" behavior arising from a temperature-dependent *increase* in k_{fold} and *decrease* in k_{unfold}, respectively.

3.2. Mg^{2+} Effects on the Temperature Dependence of Folding. Previous studies have shown that docking between the loops L1 and L3 of the manganese riboswitch requires binding of at least one divalent cation M^{2+} (Mg^{2+} or Mn^{2+}).[25,32] It has also been shown that Mg^{2+} alone promotes manganese riboswitch folding by only occupying the non-selective binding site, leaving the Mn^{2+}-specific site open for further ligand association (Figure 1). According to previous detailed kinetic analysis,[32] the fold-like structure achieved with Mg^{2+} binding plays a crucial role in opening a conformational selection ("fold-then-bind") pathway by enhancing the Mn^{2+} ligand affinity. It is therefore useful to further explore the formation of the Mn^{2+} ligand-free folded state with single-molecule thermodynamic techniques.

From the $[Mg^{2+}]$-dependent studies, folding of the manganese riboswitch is known to be effectively promoted by millimolar levels of Mg^{2+} (Figure 3A). By visual inspection, the fraction folded increases monotonically with $[Mg^{2+}]$, gradually reaching a saturation value. The nearly linear increase of fraction folded at low $[Mg^{2+}]$ indicates only a minimal Hill cooperativity ($n \approx 1$). More quantitatively, the data can be fit to the normalized Hill equation in the form of[32,37−39]

$$\text{Fraction folded} = F_0 + (1 - F_0) \times F_s\left(\frac{[M^{2+}]^n}{K_D{}^n + [M^{2+}]^n}\right) \quad (1)$$

where F_0 and F_s are fractions of the riboswitch folded at 0 and saturation $[M^{2+}]$ (M = Mg or Mn), respectively. The Hill coefficient n is readily determined to be 1.3(2), suggesting that folding could be effectively promoted by a singly occupied 5-fold coordination Mg^{2+} binding site, in agreement with structural and kinetic characterizations in previous studies.[25,32] It is worth noting that the Hill coefficient only indicates the cooperativity in ligand (Mg^{2+})-promoted folding and need not necessarily equal the binding stoichiometry.[40] Indeed, the minor deviation of n from unity could reflect increased number of Mg^{2+} ions surrounding the riboswitch during folding, for which the effective Mg^{2+} binding constant is found to be K_D = 1.1(2) mM. To explore the thermodynamics of subsequent

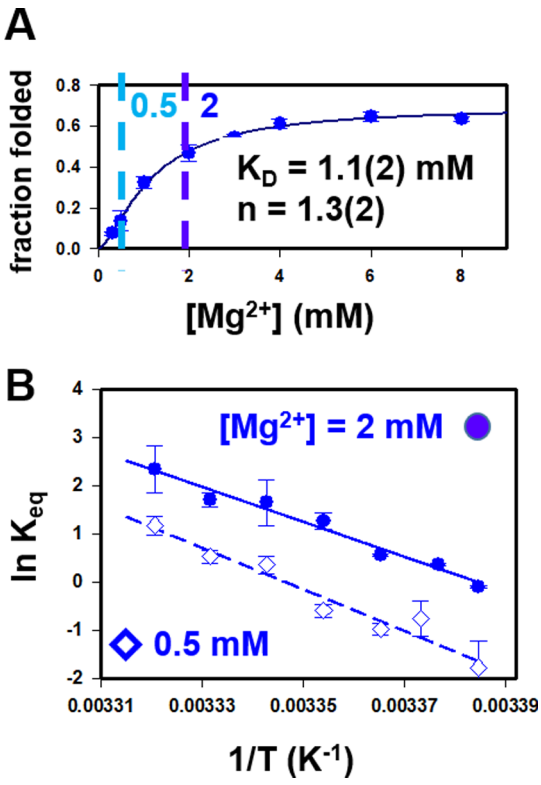

Figure 3. Mg^{2+} dependence of the manganese riboswitch folding under equilibrium conditions: (A) folded fraction as a function of $[Mg^{2+}]$; (B) van't Hoff plot for the temperature-dependent behavior of the manganese riboswitch equilibrium constant ($K_{eq} = k_{fold}/k_{unfold}$) at $[Mn^{2+}] = 0$.

Mn^{2+} binding, we therefore choose to study the temperature dependence of manganese riboswitch folding at two representative $[Mg^{2+}]$ concentrations of (i) relatively low ($[Mg^{2+}]$ = 0.5 mM < K_D) and (ii) near-saturation ($[Mg^{2+}]$ = 2 mM > K_D) levels.

The results are summarized in van't Hoff analysis (see Figure 3B), where K_{eq} is plotted logarithmically versus reciprocal temperature ($1/T$, T in kelvin). The negative slopes in the data immediately reveal that folding of the manganese riboswitch is promoted by increasing temperature. In particular, the data indicate approximately 20- and 10-fold increase in the equilibrium folding constant (K_{eq}) over a temperature change of only 10 °C, at 0.5 and 2 mM Mg^{2+}, respectively, signaling an unusually strong dependence of riboswitch conformation on temperature. More quantitatively, linear least squares fit of such van't Hoff data to

$$\ln(K_{eq}) = -\frac{\Delta H^0}{R}\frac{1}{T} + \frac{\Delta S^0}{R} \quad (2)$$

allows one to deconstruct overall free energies into enthalpic and entropic contributions, corresponding to $-\Delta H^0/R$ and $\Delta S^0/R$, respectively. The negative slope is consistent with $\Delta H^0 > 0$, which means the folding is an endothermic process and thus promoted by heat, whereas the positive intercept suggests a strong increase in entropy ($\Delta S^0 > 0$) upon folding. Such heat promoted folding (or "cold-denaturation") behavior is relatively unusual, as we more conventionally expect the folding into a more order compact state to be entropically unfavored ($\Delta S^0 < 0$) and enthalpically driven ($\Delta H^0 < 0$) by interactions such as hydrogen bonding and metal coordination.

DOI: 10.1021/acs.jpcb.9b02852
J. Phys. Chem. B 2019, 123, 5412−5422

Furthermore, the $[Mg^{2+}]$ dependence of this van't Hoff plot shows moderate changes in the slope and intercept, indicating that the Mg^{2+} dependence of folding occurs by mildly lowering the enthalpic cost ($\Delta\Delta H^0 < 0$) while decreasing the overall entropic gain ($\Delta\Delta S^0 < 0$) (Figure 3B).

At the kinetic level, we can trace the impact of temperature on equilibrium constants from the corresponding folding and unfolding rate constants. If we associate purely single-exponential kinetic behavior with a single-rate limiting TS, the detailed thermodynamic properties of this TS can be obtained from an activated TS/Eyring analysis of $\ln(k_{fold})$ or $\ln(k_{unfold})$ versus $1/T$ (see Figure 4)

$$\ln(k) = -\frac{\Delta H^{\ddagger}}{R}\frac{1}{T} + \frac{\Delta S^{\ddagger}}{R} + \ln \nu \qquad (3)$$

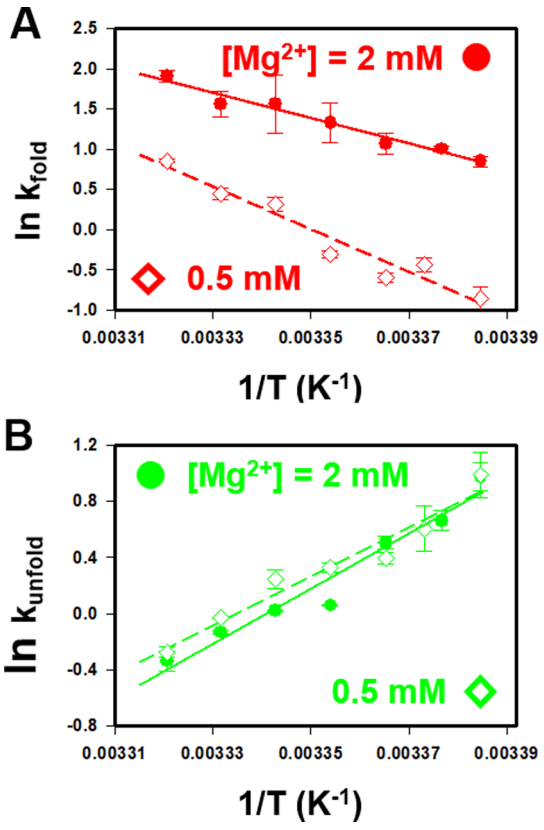

Figure 4. Kinetic effects of Mg^{2+} in an activated complex/TS theory analysis of (A) k_{fold} and (B) k_{unfold}.

In eq 3, $\Delta H^{\ddagger}$ and $\Delta S^{\ddagger}$ represent differences in enthalpy and entropy between the TS and the folded (or unfolded) state, while ν is the so-called "attempt frequency" to access the transition barrier along the reaction coordinate.[34,35,41−43] One challenge of such an activated TS analysis is that ν is generally not known a priori and often simply estimated to be of the order 10^{12} to 10^{14} s^{-1}, though the inferred entropy of the TS ($\Delta S^{\ddagger}$) depends only logarithmically on ν. However, it is worth noting that any cation-induced *changes* in this entropic barrier (i.e., $\Delta[-T\Delta S^{\ddagger}]$) exactly cancel even this weak logarithmic sensitivity and become rigorously independent of the choice of ν.[34,35]

The results of such an Eyring analysis immediately reveal several interesting features. First, a temperature rise promotes folding of the manganese riboswitch by both *increasing* k_{fold} and *decreasing* k_{unfold}, as clearly evident from the negative and positive slopes in Figure 4A,B, respectively. Second, the negative slopes for k_{fold} implies that overall folding of the manganese riboswitch is an *endothermic* process, in contrast with the more usual *exothermic* folding behavior due to formation of additional stabilizing hydrogen bonding networks. Third, increasing Mg^{2+} from 0.5 to 2 mM increases the riboswitch stability (K_{eq}) significantly but almost entirely by dramatic enhancement in k_{fold} (Figure 4A) with relatively little change on k_{unfold} (Figure 4B). However, even though k_{fold} is uniformly larger under high $[Mg^{2+}]$ conditions, it is also much less temperature sensitive than at low $[Mg^{2+}]$. Conversely, the temperature dependence of k_{unfold} is almost completely insensitive to $[Mg^{2+}]$, which echoes a similar lack of $[Mg^{2+}]$ dependence to unfolding rate constants observed from the previous study at room temperature.[32] Simply summarized, these results suggest that Mg^{2+} promotes the stability of the folded riboswitch structure predominantly by *lowering* both the folded and TS free energies by equivalent amounts, thereby permitting k_{fold} and k_{unfold} to be strongly *increased* and *largely unaffected*, respectively.

3.3. Mn^{2+} Effects on the Temperature Dependence of Folding. The $[Mn^{2+}]$-dependent folding data suggests a positive cooperativity of Mn^{2+}, whereby the fraction folded increases nearly quadratically at low $[Mn^{2+}]$ and gradually reaches saturation (Figure 5A). By Hill analysis, the cooperativity is found to be n = 1.7(2), consistent with the presence of two M^{2+} binding sites determined by X-ray structural studies.[25] Deviation of the Hill coefficient from 2 can

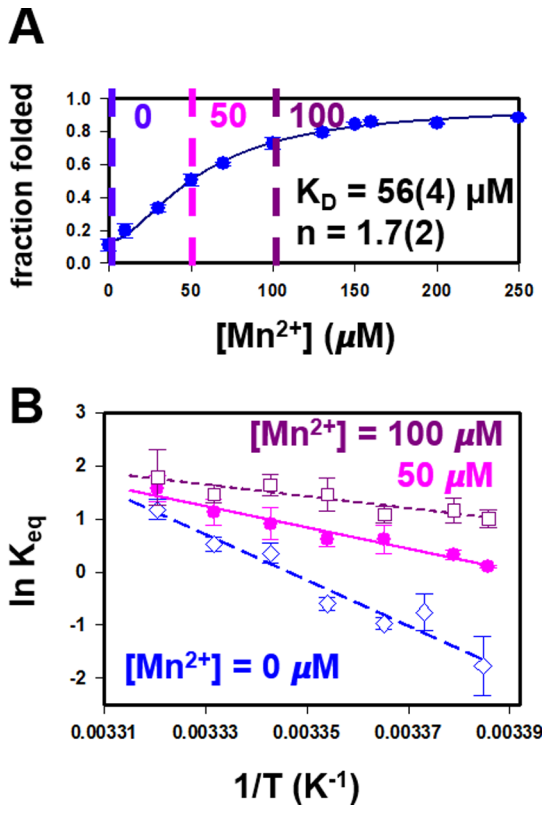

Figure 5. Mn^{2+} effects on manganese riboswitch folding under equilibrium conditions: (A) folded fraction as a function of $[Mn^{2+}]$; (B) van't Hoff plot of temperature-dependent manganese riboswitch folding at $[Mg^{2+}]$ = 0.5 mM.

DOI: 10.1021/acs.jpcb.9b02852
J. Phys. Chem. B 2019, 123, 5412−5422

be understood as arising from the nonselective cation site already being partially occupied by Mg^{2+} under near physiological conditions ($[Mg^{2+}] \approx 0.5$ mM).[32] More importantly, the effective binding constant K_D for Mn^{2+} is determined to achieve a much tighter value of 56(4) μM. We thus choose to explore the temperature-dependent rate processes at three representative $[Mn^{2+}]$ conditions corresponding to folding at (i) far below (0 μM), (ii) comparable with (50 μM), and (iii) above (100 μM) the value of K_D, respectively.

From van't Hoff analyses summarized in Figure 5B, the folding equilibria under all three cation conditions are clearly shown to be endothermic (negative slopes) and thereby promoted by increasing temperature. Furthermore, the positive intercepts indicate that folding increases the overall entropy ($\Delta S^0 > 0$) of the system. However, the manganese riboswitch reveals an unconventional heat-promoted folding behavior with a surprising sensitivity to $[Mn^{2+}]$. Specifically as $[Mn^{2+}]$ *increases*, the magnitudes of both the van't Hoff slopes and intercepts *decrease*. The net effect of Mn^{2+} on manganese riboswitch folding would therefore appear to be a simultaneous *reduction* in ΔH^0 and ΔS^0. Although more work need to be carried out, this would at least be consistent with a more common physical scenario of cation binding resulting in enthalpic stabilization ($\Delta\Delta H^0 < 0$) and yet added entropic cost ($\Delta[-T\Delta S^0] > 0$), largely caused by loss in translational entropy of the ligand.[44−46]

From the corresponding temperature-dependent folding/unfolding kinetics summarized in Figure 6, a rise in temperature promotes the overall manganese riboswitch folding once again by increasing k_{fold} and decreasing k_{unfold}. From the Eyring plots, k_{fold} (Figure 6A) becomes less sensitive to temperature, with the overall rate constant increasing but slope magnitudes decreasing dramatically with increasing $[Mn^{2+}]$. This would be consistent with any enthalpic barrier between the unfolded state and TS being lowered by increasing Mn^{2+}. The intercept, on the other hand, also decreases ($\Delta[-T\Delta S^0] > 0$) with increasing Mn^{2+}, suggesting that any entropy gain achieved during folding is mitigated by Mn^{2+}. Finally, both Eyring analysis slopes and intercepts for k_{unfold} are observed to decrease with increasing $[Mn^{2+}]$ conditions. In summary, the effect of Mn^{2+} on the kinetics would appear to lower the enthalpic barrier to folding and yet also contribute to entropically destabilizing the folded configuration.

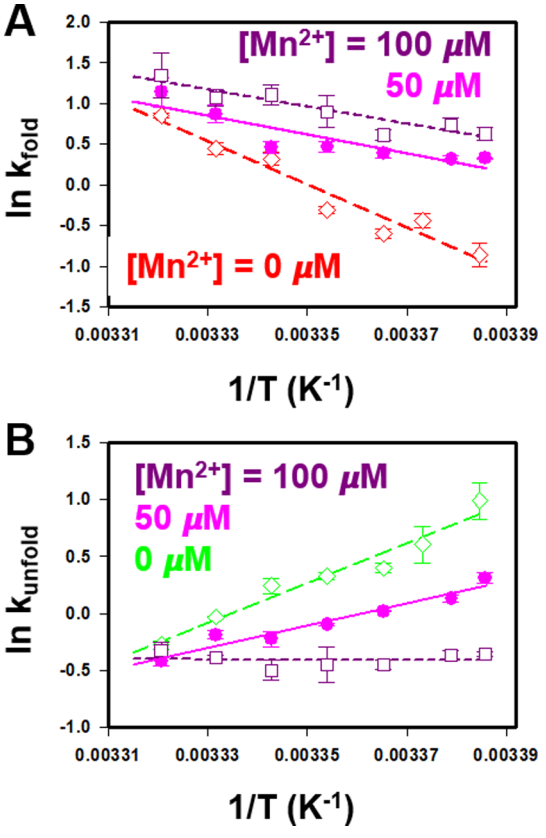

Figure 6. Kinetic dependence of Mn^{2+} in an activated complex/TS theory analysis of (A) k_{fold} and (B) k_{unfold}.

4. DISCUSSION

4.1. Unconventional Temperature Response of Manganese Riboswitch Folding. The combination of hydrogen bonding, coulombic interactions (both attractive and repulsive), and water hydration often cause nucleic acid biomolecules to spontaneously rearrange into a more ordered and compact conformation.[7,8] As a result, the conventional thermodynamic paradigm for RNA folding is an enthalpically driven process ($\Delta H^0 < 0$) but with appreciable increase in free energy due to entropic penalty in the final state ($-T\Delta S^0 > 0$). In the current studies, folding of the manganese riboswitch has been shown to be strongly promoted by increasing temperature. The negative slopes and positive intercepts in the van't Hoff plots under all Mg^{2+} and Mn^{2+} conditions indicate that folding occurs spontaneously, made possible by *entropic gain*, competing against an unfavorable *enthalpic penalty*. Though such temperature-promoted folding ("cold denaturation") seems at first counterintuitive, such behavior has nonetheless been discovered in many proteins, with the phenomenon often linked to change in solvent exposed area during folding,[47−49] for which largely entropically driven hydrophobic and hydrophilic interactions play the dominant role.

The thermodynamic analysis of Sections 3.2 and 3.3 clearly reveals that both enthalpy and entropy of the *system* (i.e., RNA construct *plus* surrounding solvent environment) increase with folding of the manganese riboswitch, with a large entropic contribution ($-T\Delta S$) compensating and even dominating free-energy stabilization of the more structured conformation. Previous studies indicate that variation in solvent exposure along the folding coordinate plays an important role in cold denaturation,[47−49] which in turn results in significant solvent impact on the equilibrium behavior. In the manganese riboswitch, the two M^{2+} binding sites are rich in phosphate groups and are highly negatively charged (Figure 1B). When such a charged species is placed in aqueous solution, the water molecules orient to lower the enthalpy ($\Delta H^0 < 0$), with water ordering, resulting in a large entropy decrease for the solvent system ($\Delta S^0 < 0$), a process known as hydration.[50,51] When the manganese riboswitch folds, the highly charged regions of RNA become less accessible to water due to partial neutralization by counterions. Thus, the reverse "dehydration" process can occur during the folding event due to water expulsion around the highly charged binding sites. If such dehydration effects predominate over intramolecular hydrogen bonding in the RNA construct, this could thereby result in (i) a large enthalpic cost ($\Delta H^0 > 0$) balanced by (ii) entropically driven folding ($\Delta S^0 > 0$). Note that the ion association (Mn^{2+}

DOI: 10.1021/acs.jpcb.9b02852
J. Phys. Chem. B 2019, 123, 5412−5422

or Mg^{2+}) during the manganese riboswitch folding may also contribute significantly to the dehydration entropy and enthalpy ($\Delta H^0 > 0$, $\Delta S^0 > 0$). Such effects can be compensated by the phosphate contacts primarily through charge neutralization, coordination bonding ($\Delta H^0 < 0$), ordering of the binding site, and loss in translational entropy ($\Delta S^0 < 0$). Because the manganese riboswitch folds into a more ordered state upon metal binding, we would expect both ΔH^0 and ΔS^0 for the construct to be less than zero. However, it is the total enthalpies and entropies of the system (RNA plus buffer solution) that is observed, likely dominated by the hydration process and solvent reorganization. For Mn^{2+} binding to the Mn^{2+}-specific site,[25,32] the process can therefore quite understandably result in lowering both the enthalpic cost and entropic gain ($\Delta(\Delta H^0) < 0$, $\Delta(\Delta S^0) < 0$), consistent with our observations in Figure 7B.

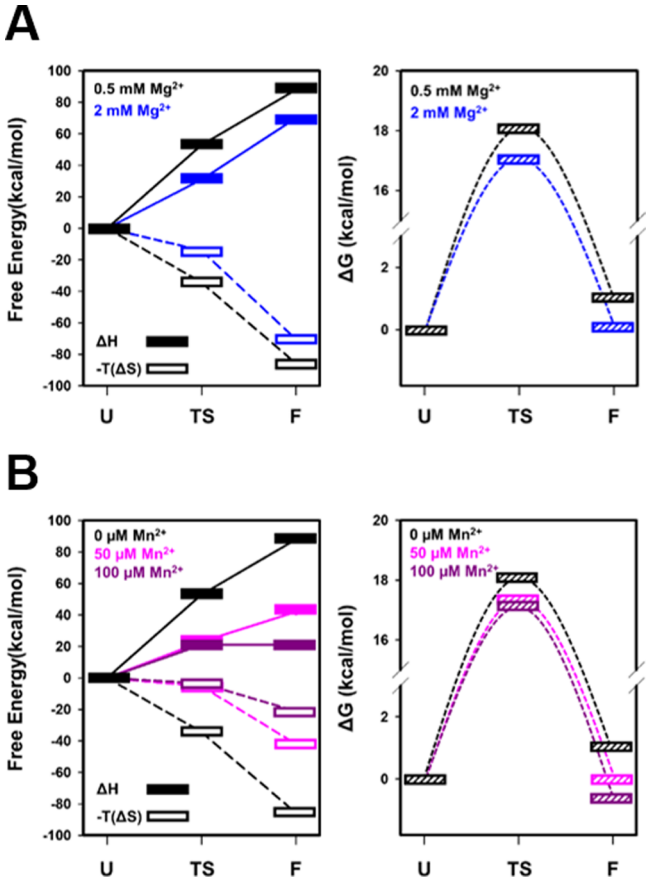

Figure 7. Folding free-energy landscapes of the manganese riboswitch: (A) Mg^{2+} effects on enthalpic and entropy contributions (left) and the overall free energy (right); (B) Mn^{2+} effects on enthalpic and entropy contributions (left) and the overall free energy (right). Note that although there is no information on changes in absolute free energies with cation conditions, the unfolded state (U) is conventionally referenced to zero free energy in both plots.

4.2. Temperature Response of RNA. Although cold denaturation (or heat-promoted folding) has been widely explored in proteins, it is much less commonly observed in RNA. One such RNA system known to exhibit heat-promoted folding is the hammerhead ribozyme,[47,48] for which temperature-dependent folding of the three-way junction has been investigated with circular dichroism (CD) over a wide range of temperature. Interestingly, the studies reveal that the three-way junction folded structure is stabilized with increasing temperature at relatively low temperature, but that this thermal stabilization of folding reverses at a critical temperature. In another recent study of the adenine-sensing riboswitch, it was shown by NMR spectroscopy that achievement of the ligand-free folded conformation is also promoted by temperature increase.[52] Despite only relatively few direct measurements of temperature-responsive RNA folding, the thermodynamic parameters for ligand-mediated riboswitch folding (without information in temperature dependence) can be estimated from isothermal titration calorimetry as well as other temperature-dependent binding studies because ligand binding is always accompanied by conformational changes in the RNA riboswitch. From literature search over 17 classes of riboswitches/ribozymes that respond to various ligands and substrates,[38,53−77] nine appeared to exhibit entropically favored binding ($\Delta S^0 > 0$),[53−62] indicating that configurational entropy of the solvent can dominate the folding entropy of the riboswitch construct. Furthermore, four out of these nine are also found to be endothermic ($\Delta H^0 > 0$),[53−58] similar to the manganese riboswitch behavior. Thus, one is led to speculate that cold denaturation might not actually be such an uncommon tertiary binding/folding strategy in RNA. In fact, RNAs are structurally polyanion electrolytes that interact strongly with water; as a result, thermodynamic free energies for RNA folding might reflect even greater sensitivity to the solvent and buffer system than for proteins.[7,15,16] This would appear likely to have evolutionary consequences. Bacteria in the wild experience significant temperature fluctuations, with some thriving under extreme temperature conditions.[17−19] It is thus perhaps not surprising that temperature sensitivity may have been evolutionarily integrated into the riboswitch function.

It is also possible to take this analysis further toward understanding the biochemical role of temperature in gene regulation. For example, Mn^{2+} is known to catalyze formation of reactive oxidative species (ROS) that are particularly damaging to cells.[78,79] In this study, we have seen that the manganese riboswitch at higher temperatures transcriptionally promotes gene expression of a Mn^{2+} efflux protein, essentially by folding into an "on" conformation. Because of more active production and higher reactivity of ROS at high temperature,[80−82] such temperature dependence could be advantageous for bacteria survival as a protective mechanism reducing cellular [Mn^{2+}]. Indeed, bacteria have been shown to exploit temperature control in gene regulation, as evident in so-called "RNA thermometers,"[22,23] that is, small mRNA elements that structurally respond to temperature in regulation of translational efficiency. Because RNA structures are highly responsive to temperature, it is interesting to speculate that *cation* plus *environmental temperature* modulation of a specific RNA conformation could reflect a more general strategic example of *multicomponent sensitivity* in riboswitch gene regulation.

4.3. Reconstructing Folding Free-Energy Landscapes from Temperature-Dependent Kinetics. The thermodynamic/kinetic parameters obtained from the current van't Hoff and Eyring analyses can provide particularly invaluable information on pieces of the overall free-energy landscape for folding of the manganese riboswitch. We note that in the resulting energy diagrams (Figure 7), the errors (with proper propagation) in enthalpic (ΔH) and entropic ($-T\Delta S$) contributions typically range from 5 to 10 kcal/mol due to fitting within a limited temperature window. Nonetheless,

DOI: 10.1021/acs.jpcb.9b02852
J. Phys. Chem. B 2019, 123, 5412−5422

these errors are relatively small compared to (i) energy differences between unfolded, folded, and TS and (ii) salt-based M^{2+} effects, which are each >20 kcal/mol. As a result, the overall free-energy changes (ΔG) directly obtained from equilibrium (K_{eq}) and rate constant (k) data have $\sigma \leq 0.3$ kcal/mol in uncertainties (standard deviation of the mean). For Mg^{2+} dependence, Figure 7A immediately reveals that the enthalpic (ΔH) and entropic ($-T\Delta S$) contributions to the free energy (ΔG) for both the TS and folded (F) state confirmations move synchronously up/down with increasing Mg^{2+} in a clearly anticorrelated fashion. This notable level of synchrony suggests that the impact of Mg^{2+} is primarily on the enthalpy/entropy of the unfolded state (U), as shifts in only U would maintain all relative free-energy spacings between the TS and F conformations. Such a strong dependence of unfolded structure free energies on $[Mg^{2+}]$ can be rationalized as arising from differential Mg^{2+} occupancy at the nonselective M^{2+} binding site, as these experiments are performed at Mg^{2+} concentrations, appreciably below (0.5 mM) and above (2 mM) the effective binding affinity (K_D = 1.1 mM). Simply stated, because M^{2+} binding is essential for riboswitch folding,[32] the free-energy differences between the anticorrelated TS and F states are insensitive to $[Mg^{2+}]$ due to the fact that they are both associated with one Mg^{2+}. Thus, the Mg^{2+}-mediated manganese riboswitch folding thermodynamic plots in Figure 7A reveal that Mg^{2+} binding must occur while the construct is still mostly *unfolded*. In agreement with the previous kinetic studies, this is consistent with an IF (i.e., "bind-then-fold") mechanism,[30,32,33] whereby prior binding of the ligand is required to achieve the correct folding behavior. We note that such information can be gleaned from the plots even in the absence of any knowledge about *absolute* free energies, which are not accessible (e.g., the free energy for the U state is referenced to zero at all cation conditions).

Similarly for $[Mn^{2+}]$-dependent riboswitch folding (Figure 7B), the entropy and enthalpy of the TS and F states are both significantly shifted with increasing Mn^{2+} concentration. Overall, as $[Mn^{2+}]$ increases, the enthalpic (ΔH) and entropic ($-T\Delta S$) contributions bifurcate systematically. Such effects are in agreement with ligand-binding models, where the enthalpic gain (from Mn^{2+} coordination) is accompanied by entropic loss largely in translational entropy of the ligand and higher degree of ordering at the binding site.[44−46] Interestingly, however, there is also a strong nonlinear saturation dependence of these effects on $[Mn^{2+}]$. For example, the TS free energy changes significantly between 0 and 50 μM of Mn^{2+} and yet remains essentially constant with an additional aliquot of 50 μM Mn^{2+} (100 μM in total). This behavior is likely due to the fact that Mn^{2+} promotes achievement of the TS state via different occupancies of the two M^{2+} binding sites. Indeed, the largest free-energy effects between conditions of 50 and 100 μM Mn^{2+} appear in the folded (F) state but now with negligible changes in the TS and U conformations. Much as invoked above for Mg^{2+} dependence, this can be simply rationalized by the folded state existing with two different metal occupancies of the two binding sites: one M^{2+} (M = Mn or Mg) binding or two M^{2+} binding with at least one Mn^{2+}. The Mn^{2+} effect of $\Delta(\Delta H^0) < 0$ and $\Delta(\Delta S^0) < 0$ is again consistent with increased Mn^{2+} binding. Although the manganese riboswitch is known to fold via an IF (bind-then-fold) mechanism with at least one M^{2+} binding in the unfolded state,[32] the ability of Mn^{2+} to directly bind to a (pre)folded conformation (e.g., Mg^{2+}-bound folded conformation with an unoccupied Mn^{2+} binding site) and thereby stabilize the folding equilibrium is consistent with a conformational selection (CS, fold-then-bind) mechanism,[30,32,33] whereby the RNA dynamically samples many different configurations, while the ligand binds only to those constructs with a preformed Mn^{2+} binding site. To summarize, the thermodynamic analysis of the rate and equilibrium data reveals that the manganese riboswitch folds through an IF mechanism via early Mg^{2+} association with U. Conversely, Mn^{2+} binds to a prefolded ligand-free riboswitch structure to stabilize the folding equilibrium (i.e., in support of a CS mechanism), as evidenced by selective effects of Mn^{2+} > 50 μM on the free energy of the folded (F) configuration. We note that although our mechanistic interpretation of the thermodynamic data is motivated and strongly supported by the previous work, molecular dynamics simulations would be extremely valuable and could provide additional confirmation. Finally, it is worth emphasizing that such Mn^{2+} and Mg^{2+} ligand binding shifts in the enthalpic and entropic contributions are all anticorrelated and very finely balanced to yield only relatively small differences (of order 1 kcal/mol) in the overall free energies for the folded versus unfolded states of the riboswitch. This allows for strong environmental regulation of the kinetic rates and time constants for riboswitch folding, with only relatively small changes in the overall folding stability. Such a cationic modulation of the folding time constant behavior could be relevant in cotranscriptional folding dynamics and gene regulation strategies.[30,31]

5. SUMMARY AND CONCLUSIONS

The temperature dependence of manganese riboswitch folding has been explored in detail by confocal smFRET experiments. The folded manganese riboswitch conformation is found to be strongly stabilized by temperature, which from a kinetic perspective occurs via simultaneous increase (decrease) in the folding (unfolding) unimolecular rate constants, respectively. A thermal van't Hoff analysis of the equilibrium constant reveals that folding is strongly disfavored enthalpically (ΔH^0) while favored with significant and closely balanced entropic contributions ($-T\Delta S^0$) to yield an overall ΔG^0. This is in clear contrast with the more conventional behavior of ligand-promoted folding behavior of entropically disfavored folding into a compact state driven by enthalpic energy release.[9,10] Such temperature-promoted folding (or equivalently, cold denaturation) can result from the change in ionic hydration/dehydration and hydrophilic/hydrophobic interactions, highlighting the crucial importance of *solvent* contributions to the overall free-energy change in an RNA folding event. Moreover, we speculate that such a less conventional thermophilic response of the manganese riboswitch may provide an additionally useful survival mechanism for successful bacterial proliferation in a fluctuating temperature environment, suggesting a mechanism by which temperature may be more widely incorporated into riboswitch gene regulation. In Mg^{2+}-mediated folding, Mg^{2+} is found to mainly affect the free energy of the unfolded (U) state, consistent with the unfolded structure having 0 or 1 Mg^{2+} occupancy and yet with the ones binding to a single Mg^{2+} able to access the TS and thereby achieve a fully folded structure. Such binding of a single Mg^{2+} prior to the TS supports the predominant existence of an IF ("bind-then-fold") mechanism for Mg^{2+}-promoted folding. For Mn^{2+}-mediated folding, by way of contrast, Mn^{2+} is found to significantly shift the relative free energies of *both* the TS and

DOI: 10.1021/acs.jpcb.9b02852
J. Phys. Chem. B 2019, 123, 5412−5422

folded (F) states. This sensitivity to [Mn^{2+}] is consistent with the folded state of the riboswitch associating different numbers of Mn^{2+} into its two (selective and nonselective) binding sites, which would provide support for a conformational selection ("fold-then-bind") pathway. Such a combined thermal and cation sensitivity to modulation of the riboswitch folding pathway offers distinctly new opportunities for evolutionary adaptation and flexibility of the manganese riboswitch to various environmental conditions.

AUTHOR INFORMATION

Corresponding Author

*E-mail: djn@jila.colorado.edu.

ORCID

David J. Nesbitt: 0000-0001-5365-1120

Notes

The authors declare no competing financial interest.

ACKNOWLEDGMENTS

The authors would like to thank Jake Polaski and Professor Robert T. Batey for help with synthesis of the RNA constructs, labeling with Cy3/Cy5 FRET dye pairs, as well as many insightful discussions. Funding for this work was provided by the National Science Foundation (CHE-1665271, PHY 1734006) and the National Institute for Standards and Technology, with initial support by the W. M. Keck Foundation Initiative in RNA sciences at the University of Colorado, Boulder.

REFERENCES

(1) Mironov, A. S.; Gusarov, I.; Rafikov, R.; Lopez, L. E.; Shatalin, K.; Kreneva, R. A.; Perumov, D. A.; Nudler, E. Sensing Small Molecules by Nascent RNA. *Cell* **2002**, *111*, 747−756.

(2) Nahvi, A.; Sudarsan, N.; Ebert, M. S.; Zou, X.; Brown, K. L.; Breaker, R. R. Genetic Control by a Metabolite Binding mRNA. *Chem. Biol.* **2002**, *9*, 1043−1049.

(3) Tucker, B. J.; Breaker, R. R. Riboswitches as Versatile Gene Control Elements. *Curr. Opin. Struct. Biol.* **2005**, *15*, 342−348.

(4) Serganov, A.; Nudler, E. A Decade of Riboswitches. *Cell* **2013**, *152*, 17−24.

(5) Roth, A.; Breaker, R. R. The Structural and Functional Diversity of Metabolite-Binding Riboswitches. *Annu. Rev. Biochem.* **2009**, *78*, 305−334.

(6) Garst, A. D.; Edwards, A. L.; Batey, R. T. Riboswitches: Structures and Mechanisms. *Cold Spring Harbor Perspect. Biol.* **2011**, *3*, a003533.

(7) Brady, G. P.; Sharp, K. A. Entropy in Protein Folding and in Protein—Protein Interactions. *Curr. Opin. Struct. Biol.* **1997**, *7*, 215−221.

(8) Onuchic, J. N.; Wolynes, P. G. Theory of Protein Folding. *Curr. Opin. Struct. Biol.* **2004**, *14*, 70−75.

(9) Draper, D. E. Strategies for RNA Folding. *Trends Biochem. Sci.* **1996**, *21*, 145−149.

(10) Dill, K. A. Dominant Forces in Protein Folding. *Biochemistry* **1990**, *29*, 7133−7155.

(11) Schildkraut, C.; Lifson, S. Dependence of the Melting Temperature of DNA on Salt Concentration. *Biopolymers* **1965**, *3*, 195−208.

(12) Donovan, J. W.; Mapes, C. J.; Davis, J. G.; Garibaldi, J. A. A Differential Scanning Calorimetric Study of the Stability of Egg White to Heat Denaturation. *J. Sci. Food Agric.* **1975**, *26*, 73−83.

(13) Privalov, P. L. Cold Denaturation of Protein. *Crit. Rev. Biochem. Mol. Biol.* **1990**, *25*, 281−306.

(14) Hatley, R. H. M.; Franks, F. Cold Destabilisation of Enzymes. *Faraday Discuss.* **1992**, *93*, 249−257.

(15) Makhatadze, G. I.; Privalov, P. L. Contribution of Hydration to Protein Folding Thermodynamics. *J. Mol. Biol.* **1993**, *232*, 639−659.

(16) Privalov, P. L.; Makhatadze, G. I. Contribution of Hydration to Protein Folding Thermodynamics. *J. Mol. Biol.* **1993**, *232*, 660−679.

(17) Kurr, M.; Huber, R.; König, H.; Jannasch, H. W.; Fricke, H.; Trincone, A.; Kristjansson, J. K.; Stetter, K. O. Methanopyrus Kandleri, gen. and Sp. Nov. Represents a Novel Group of Hyperthermophilic Methanogens, Growing at 110°C. *Arch. Microbiol.* **1991**, *156*, 239−247.

(18) Takai, K.; Nakamura, K.; Toki, T.; Tsunogai, U.; Miyazaki, M.; Miyazaki, J.; Hirayama, H.; Nakagawa, S.; Nunoura, T.; Horikoshi, K. Cell Proliferation at 122°C and Isotopically Heavy Ch₄ Production by a Hyperthermophilic Methanogen under High-Pressure Cultivation. *Proc. Natl. Acad. Sci. U.S.A.* **2008**, *105*, 10949−10954.

(19) Mykytczuk, N. C. S.; Foote, S. J.; Omelon, C. R.; Southam, G.; Greer, C. W.; Whyte, L. G. Bacterial Growth at −15 °C; Molecular Insights from the Permafrost Bacterium Planococcus halocryophilus Or1. *ISME J.* **2013**, *7*, 1211.

(20) Hurme, R.; Rhen, M. Temperature Sensing in Bacterial Gene Regulation — What It All Boils Down To. *Mol. Microbiol.* **1998**, *30*, 1−6.

(21) Konkel, M. E.; Tilly, K. Temperature-Regulated Expression of Bacterial Virulence Genes. *Microbes Infect.* **2000**, *2*, 157−166.

(22) Narberhaus, F. Translational Control of Bacterial Heat Shock and Virulence Genes by Temperature-Sensing mRNAs. *RNA Biol.* **2010**, *7*, 84−89.

(23) Kortmann, J.; Narberhaus, F. Bacterial RNA Thermometers: Molecular Zippers and Switches. *Nat. Rev. Microbiol.* **2012**, *10*, 255.

(24) Barrick, J. E.; Corbino, K. A.; Winkler, W. C.; Nahvi, A.; Mandal, M.; Collins, J.; Lee, M.; Roth, A.; Sudarsan, N.; Jona, I.; et al. New RNA Motifs Suggest an Expanded Scope for Riboswitches in Bacterial Genetic Control. *Proc. Natl. Acad. Sci. U.S.A.* **2004**, *101*, 6421−6426.

(25) Price, I. R.; Gaballa, A.; Ding, F.; Helmann, J. D.; Ke, A. Mn^{2+}-Sensing Mechanisms of Yybp-Ykoy Orphan Riboswitches. *Mol. Cell* **2015**, *57*, 1110−1123.

(26) Dambach, M.; Sandoval, M.; Updegrove, T. B.; Anantharaman, V.; Aravind, L.; Waters, L. S.; Storz, G. The Ubiquitous Yybp-Ykoy Riboswitch Is a Manganese-Responsive Regulatory Element. *Mol. Cell* **2015**, *57*, 1099−1109.

(27) Waters, L. S.; Sandoval, M.; Storz, G. The Escherichia Coli Mntr Miniregulon Includes Genes Encoding a Small Protein and an Efflux Pump Required for Manganese Homeostasis. *J. Bacteriol.* **2011**, *193*, 5887−5897.

(28) Veyrier, F. J.; Boneca, I. G.; Cellier, M. F.; Taha, M.-K. A Novel Metal Transporter Mediating Manganese Export (MntX) Regulates the Mn to Fe Intracellular Ratio and Neisseria Meningitidis Virulence. *PLoS Pathog.* **2011**, *7*, No. e1002261.

(29) Li, C.; Tao, J.; Mao, D.; He, C. A Novel Manganese Efflux System, YebN, Is Required for Virulence by Xanthomonas Oryzae pv. Oryzae. *PLoS One* **2011**, *6*, No. e21983.

(30) Haller, A.; Soulière, M. F.; Micura, R. The Dynamic Nature of RNA as Key to Understanding Riboswitch Mechanisms. *Acc. Chem. Res.* **2011**, *44*, 1339−1348.

(31) Garst, A. D.; Batey, R. T. A Switch in Time: Detailing the Life of a Riboswitch. *Biochim. Biophys. Acta, Gene Regul. Mech.* **2009**, *1789*, 584−591.

(32) Sung, H.-L.; Nesbitt, D. J. Single Molecule Fret Kinetics of the Mn^{2+} Riboswitch: Evidence for Allosteric Mg^{2+} Control of "Induced Fit" Vs. "Conformational Selection" Folding Pathways. *J. Phys. Chem. B* **2019**, *123*, 2005.

(33) Leulliot, N.; Varani, G. Current Topics in RNA−Protein Recognition: Control of Specificity and Biological Function through Induced Fit and Conformational Capture. *Biochemistry* **2001**, *40*, 7947−7956.

(34) Fiore, J. L.; Holmstrom, E. D.; Nesbitt, D. J. Entropic Origin of Mg^{2+}-Facilitated RNA Folding. *Proc. Natl. Acad. Sci. U.S.A.* **2012**, *109*, 2902−2907.

DOI: 10.1021/acs.jpcb.9b02852
J. Phys. Chem. B 2019, 123, 5412−5422

(35) Sengupta, A.; Sung, H.-L.; Nesbitt, D. J. Amino Acid Specific Effects on RNA Tertiary Interactions: Single-Molecule Kinetic and Thermodynamic Studies. *J. Phys. Chem. B* **2016**, *120*, 10615−10627.
(36) Nicholson, D. A.; Sengupta, A.; Sung, H.-L.; Nesbitt, D. J. Amino Acid Stabilization of Nucleic Acid Secondary Structure: Kinetic Insights from Single-Molecule Studies. *J. Phys. Chem. B* **2018**, *122*, 9869−9876.
(37) Fiegland, L. R.; Garst, A. D.; Batey, R. T.; Nesbitt, D. J. Single-Molecule Studies of the Lysine Riboswitch Reveal Effector-Dependent Conformational Dynamics of the Aptamer Domain. *Biochemistry* **2012**, *51*, 9223−9233.
(38) Schroeder, K. T.; Daldrop, P.; Lilley, D. M. J. RNA Tertiary Interactions in a Riboswitch Stabilize the Structure of a Kink Turn. *Structure* **2011**, *19*, 1233−1240.
(39) Hennelly, S. P.; Novikova, I. V.; Sanbonmatsu, K. Y. The Expression Platform and the Aptamer: Cooperativity between Mg^{2+} and Ligand in the Sam-I Riboswitch. *Nucleic Acids Res.* **2013**, *41*, 1922−1935.
(40) Leipply, D.; Draper, D. E. Dependence of RNA Tertiary Structural Stability on Mg^{2+} Concentration: Interpretation of the Hill Equation and Coefficient. *Biochemistry* **2010**, *49*, 1843−1853.
(41) Szabo, A.; Schulten, K.; Schulten, Z. First Passage Time Approach to Diffusion Controlled Reactions. *J. Chem. Phys.* **1980**, *72*, 4350−4357.
(42) Zwanzig, R.; Szabo, A.; Bagchi, B. Levinthal's Paradox. *Proc. Natl. Acad. Sci. U.S.A.* **1992**, *89*, 20−22.
(43) Zhou, H.-X. Rate Theories for Biologists. *Q. Rev. Biophys.* **2010**, *43*, 219−293.
(44) Murphy, K. P.; Xie, D.; Thompson, K. S.; Amzel, L. M.; Freire, E. Entropy in Biological Binding Processes: Estimation of Translational Entropy Loss. *Proteins: Struct., Funct., Bioinf.* **1994**, *18*, 63−67.
(45) Amzel, L. M. Loss of Translational Entropy in Binding, Folding, and Catalysis. *Proteins: Struct., Funct., Bioinf.* **1997**, *28*, 144−149.
(46) Lu, B.; Wong, C. F. Direct Estimation of Entropy Loss Due to Reduced Translational and Rotational Motions Upon Molecular Binding. *Biopolymers* **2005**, *79*, 277−285.
(47) Mikulecky, P. J.; Feig, A. L. Cold Denaturation of the Hammerhead Ribozyme. *J. Am. Chem. Soc.* **2002**, *124*, 890−891.
(48) Mikulecky, P. J.; Feig, A. L. Heat Capacity Changes in RNA Folding: Application of Perturbation Theory to Hammerhead Ribozyme Cold Denaturation. *Nucleic Acids Res.* **2004**, *32*, 3967−3976.
(49) Cooper, A.; Johnson, C. M.; Lakey, J. H.; Nöllmann, M. Heat Does Not Come in Different Colours: Entropy−Enthalpy Compensation, Free Energy Windows, Quantum Confinement, Pressure Perturbation Calorimetry, Solvation and the Multiple Causes of Heat Capacity Effects in Biomolecular Interactions. *Biophys. Chem.* **2001**, *93*, 215−230.
(50) Lumry, R.; Rajender, S. Enthalpy−Entropy Compensation Phenomena in Water Solutions of Proteins and Small Molecules: A Ubiquitous Property of Water. *Biopolymers* **1970**, *9*, 1125−1227.
(51) Schmid, R.; Miah, A. M.; Sapunov, V. N. A New Table of the Thermodynamic Quantities of Ionic Hydration: Values and Some Applications (Enthalpy−Entropy Compensation and Born Radii). *Phys. Chem. Chem. Phys.* **2000**, *2*, 97−102.
(52) Reining, A.; Nozinovic, S.; Schlepckow, K.; Buhr, F.; Fürtig, B.; Schwalbe, H. Three-State Mechanism Couples Ligand and Temperature Sensing in Riboswitches. *Nature* **2013**, *499*, 355.
(53) McConnell, T. S.; Cech, T. R. A Positive Entropy Change for Guanosine Binding and for the Chemical Step in the Tetrahymena Ribozyme Reaction. *Biochemistry* **1995**, *34*, 4056−4067.
(54) Kuo, L.; Cech, T. R. Conserved Thermochemistry of Guanosine Nucleophile Binding for Structurally Distinct Group I Ribozymes. *Nucleic Acids Res.* **1996**, *24*, 3722−3727.
(55) Huang, L.; Serganov, A.; Patel, D. J. Structural Insights into Ligand Recognition by a Sensing Domain of the Cooperative Glycine Riboswitch. *Mol. Cell* **2010**, *40*, 774−786.
(56) Trausch, J. J.; Ceres, P.; Reyes, F. E.; Batey, R. T. The Structure of a Tetrahydrofolate-Sensing Riboswitch Reveals Two Ligand Binding Sites in a Single Aptamer. *Structure* **2011**, *19*, 1413−1423.
(57) Burnouf, D.; Ennifar, E.; Guedich, S.; Puffer, B.; Hoffmann, G.; Bec, G.; Disdier, F.; Baltzinger, M.; Dumas, P. Kinitc: A New Method for Obtaining Joint Thermodynamic and Kinetic Data by Isothermal Titration Calorimetry. *J. Am. Chem. Soc.* **2012**, *134*, 559−565.
(58) Baird, N. J.; Ferre-D'Amare, A. R. Modulation of Quaternary Structure and Enhancement of Ligand Binding by the K-Turn of Tandem Glycine Riboswitches. *RNA* **2013**, *19*, 167−176.
(59) Gilbert, S. D.; Rambo, R. P.; Van Tyne, D.; Batey, R. T. Structure of the Sam-Ii Riboswitch Bound to S-Adenosylmethionine. *Nat. Struct. Mol. Biol.* **2008**, *15*, 177.
(60) Ren, A.; Rajashankar, K. R.; Patel, D. J. Fluoride Ion Encapsulation by Mg^{2+} Ions and Phosphates in a Fluoride Riboswitch. *Nature* **2012**, *486*, 85.
(61) Ren, A.; Patel, D. J. C-Di-Amp Binds the Ydao Riboswitch in Two Pseudo-Symmetry−Related Pockets. *Nat. Chem. Biol.* **2014**, *10*, 780.
(62) Ren, A.; Rajashankar, K. R.; Patel, D. J. Global RNA Fold and Molecular Recognition for a Pfl Riboswitch Bound to Zmp, a Master Regulator of One-Carbon Metabolism. *Structure* **2015**, *23*, 1375−1381.
(63) Stoddard, C. D.; Gilbert, S. D.; Batey, R. T. Ligand-Dependent Folding of the Three-Way Junction in the Purine Riboswitch. *RNA* **2008**, *14*, 675−684.
(64) Wickiser, J. K.; Cheah, M. T.; Breaker, R. R.; Crothers, D. M. The Kinetics of Ligand Binding by an Adenine-Sensing Riboswitch. *Biochemistry* **2005**, *44*, 13404−13414.
(65) Gao, A.; Serganov, A. Structural Insights into Recognition of C-Di-Amp by the Ydao Riboswitch. *Nat. Chem. Biol.* **2014**, *10*, 787.
(66) Wood, S.; Ferré-D'Amaré, A. R.; Rueda, D. Allosteric Tertiary Interactions Preorganize the C-Di-Gmp Riboswitch and Accelerate Ligand Binding. *ACS Chem. Biol.* **2012**, *7*, 920−927.
(67) Kang, M.; Eichhorn, C. D.; Feigon, J. Structural Determinants for Ligand Capture by a Class Ii $Preq_1$ Riboswitch. *Proc. Natl. Acad. Sci. U.S.A.* **2014**, *111*, No. E663.
(68) Wickiser, J. K.; Winkler, W. C.; Breaker, R. R.; Crothers, D. M. The Speed of RNA Transcription and Metabolite Binding Kinetics Operate an Fmn Riboswitch. *Mol. Cell* **2005**, *18*, 49−60.
(69) Baird, N. J.; Ferre-D'Amare, A. R. Idiosyncratically Tuned Switching Behavior of Riboswitch Aptamer Domains Revealed by Comparative Small-Angle X-Ray Scattering Analysis. *RNA* **2010**, *16*, 598−609.
(70) Batey, R. T.; Gilbert, S. D.; Montange, R. K. Structure of a Natural Guanine-Responsive Riboswitch Complexed with the Metabolite Hypoxanthine. *Nature* **2004**, *432*, 411.
(71) Gilbert, S. D.; Stoddard, C. D.; Wise, S. J.; Batey, R. T. Thermodynamic and Kinetic Characterization of Ligand Binding to the Purine Riboswitch Aptamer Domain. *J. Mol. Biol.* **2006**, *359*, 754−768.
(72) Edwards, A. L.; Reyes, F. E.; Heroux, A.; Batey, R. T. Structural Basis for Recognition of S-adenosylhomocysteine by Riboswitches. *RNA* **2010**, *16*, 2144−2155.
(73) Pikovskaya, O.; Polonskaia, A.; Patel, D. J.; Serganov, A. Structural Principles of Nucleoside Selectivity in a 2′-Deoxyguanosine Riboswitch. *Nat. Chem. Biol.* **2011**, *7*, 748.
(74) Wilson, R. C.; Smith, A. M.; Fuchs, R. T.; Kleckner, I. R.; Henkin, T. M.; Foster, M. P. Tuning Riboswitch Regulation through Conformational Selection. *J. Mol. Biol.* **2011**, *405*, 926−938.
(75) Muller, M.; Weigand, J. E.; Weichenrieder, O.; Suess, B. Thermodynamic Characterization of an Engineered Tetracycline-Binding Riboswitch. *Nucleic Acids Res.* **2006**, *34*, 2607−2617.
(76) Li, Y.; Bevilacqua, P. C.; Mathews, D.; Turner, D. H. Thermodynamic and Activation Parameters for Binding of a Pyrene-Labeled Substrate by the Tetrahymena Ribozyme: Docking Is Not Diffusion-Controlled and Is Driven by a Favorable Entropy Change. *Biochemistry* **1995**, *34*, 14394−14399.

DOI: 10.1021/acs.jpcb.9b02852
J. Phys. Chem. B 2019, 123, 5412−5422

(77) Kulshina, N.; Edwards, T. E.; Ferre-D'Amare, A. R. Thermodynamic Analysis of Ligand Binding and Ligand Binding-Induced Tertiary Structure Formation by the Thiamine Pyrophosphate Riboswitch. *RNA* **2010**, *16*, 186−196.
(78) Ali, S. F.; Duhart, H. M.; Newport, G. D.; Lipe, G. W.; Slikker, W. Manganese-Induced Reactive Oxygen Species: Comparison between Mn^{+2} and Mn^{+3}. *Neurodegeneration* **1995**, *4*, 329−334.
(79) Brenneman, K. A.; Cattley, R. C.; Ali, S. F.; Dorman, D. C. Manganese-Induced Developmental Neurotoxicity in the Cd Rat: Is Oxidative Damage a Mechanism of Action? *NeuroToxicology* **1999**, *20*, 477−487.
(80) Sairam, R. K.; Deshmukh, P. S.; Shukla, D. S. Tolerance of Drought and Temperature Stress in Relation to Increased Antioxidant Enzyme Activity in Wheat. *J. Agron. Crop Sci.* **1997**, *178*, 171−178.
(81) Sairam, R. K.; Srivastava, G. C.; Saxena, D. C. Increased Antioxidant Activity under Elevated Temperatures: A Mechanism of Heat Stress Tolerance in Wheat Genotypes. *Biol. Plant.* **2000**, *43*, 245−251.
(82) Lushchak, V. I.; Bagnyukova, T. V. Temperature Increase Results in Oxidative Stress in Goldfish Tissues. 2. Antioxidant and Associated Enzymes. *Comp. Biochem. Physiol., C: Comp. Pharmacol.* **2006**, *143*, 36−41.

DOI: 10.1021/acs.jpcb.9b02852
J. Phys. Chem. B 2019, 123, 5412−5422